Role of Shocks in Transonic/Supersonic Compressor Rotor Flutter

O. O. Bendiksen*
Princeton University, Princeton, New Jersey

An investigation of the influence of shock motion on flutter of rotors and cascades is presented. The present paper illustrates how a perturbation scheme can be used to calculate the nonlinear effects due to thickness, camber, and incidence to second order in a perturbation parameter. An approximate theory is also given, that accounts for the first-order quasisteady effects of shock motion and also allows experimentally determined shock structures and parameters to be used. The unsteady aerodynamic forces resulting from shock movements are shown to have a pronounced effect on the flutter boundaries of cascades representative of large fan rotors. Both stabilizing and destabilizing effects are observed, depending on interblade phase angle and shock structure. At low reduced frequencies, the shock-induced loads can destabilize bending oscillations sufficiently to cause single-degree-of-freedom bending flutter. It is also possible to explain the stabilizing effect of the back pressure on supersonic rotor flutter, as observed experimentally.

Nomenclature

a = speed of sound; also location of pitching axis, Eq. (8)
c = $2b$ = blade chord
$C_{Lv}, C_{L\alpha}, C_{Mv}, C_{M\alpha}$ = force and moment coefficients, Eqs. (26), (27)
h = bending deflection, positive down
k = $\omega b/U$ = reduced frequency
$\bar{k}$ = kM/β^2
L = lift per unit span, positive up
m = mass per unit span of blade
M = moment per unit span, about midchord, positive clockwise; also Mach number
M_2 = cascade exit Mach number
N = $(\gamma+1)M^2/(2\beta^2)$; also number of blades in rotor
p = static pressure
Δp_s = $p_3 - p_1$ = pressure jump at shock reflection, Fig. 3
q = $\nabla\Phi$ = velocity vector
u,v = perturbation velocities in x,y directions
U_∞ = freestream velocity at upstream infinity
s = blade spacing (Fig. 1)
s_1 = $s\sin\theta$
s_2 = $s\cos\theta$
t = time
$x,y; x',y'$ = cascade coordinate systems (Fig. 1)
x_r = mean location of shock reflection point
$x_s, \Delta x_s$ = instantaneous shock reflection point and its oscillation amplitude, respectively
α = angle of attack; also torsional deflection
β = $\sqrt{M^2-1}$
γ = ratio of specific heats of air
θ = stagger angle
θ_2 = flow deflection at trailing edge
μ = $m/\pi\rho b^2$ = mass ratio of blade
ρ = air density
σ = interblade phase angle
ν = $\beta\bar{k}/b$
ϕ = steady (mean) perturbation potential
$\tilde{\phi}$ = unsteady perturbation potential about mean flow
Φ = total potential
ϕ_s = phase angle of shock motion
ω = circular frequency
Ω = $\sigma + \bar{s}_1\bar{k}M$

Superscripts and Subscripts

$(\bar{\ })$ = nondimensional quantity: lengths with respect to semichord b, velocities with respect to U_∞, pressure with respect to $\rho_\infty U_\infty^2$
0 = amplitude of harmonic quantity
∞ = conditions at upstream infinity (freestream)
s = quantity associated with shock wave

I. Introduction

TRANSONIC compressor rotors are susceptible to a number of aeroelastic instabilities, of which supersonic flutter is now recognized as one of the most dangerous. Because of its practical importance, a number of investigators have considered this problem over the past decade. Most of the studies have been based on supersonic cascade theories, as in Refs. 1-5, with the flow linearized about the uniform steady flow. In this case, the unsteady lifts and moments are not affected, to first order, by thickness, camber, and incidence and, therefore, the blades may be treated as flat plates aligned with the upstream flow.

Although linearized cascade theories have been successful in predicting some of the overall characteristics of supersonic rotor flutter, a number of experimentally observed features remain unexplained. This is often interpreted as an indication of the inherent limitations of flat-plate analyses and that the effect of blade geometry and angle of attack should be taken into account. While recent studies[6,7] have demonstrated the importance of these effects for *subsonic* cascades, published result for supersonic cascades[8-10] are still too incomplete to draw definite conclusions. The approximate analysis in Ref. 9, however, does suggest that blade geometry and loading are also important in the supersonic case.

The purpose of this paper is to illustrate the crucial role that shock motion plays in the transonic/supersonic rotor flutter problem. Since the mean strength of these shocks is related to the blade geometry (thickness, camber) and angle of attack, the unsteady forces induced by the shocks and their reflections represent an important coupling effect between the steady and the unsteady flow perturbations. For thin blading with small camber typical of the supersonic tip region of fans, this shock-induced coupling appears to be the dominant coupling effect as far as aeroelastic stability is concerned.

Received April 17, 1985; revision received Oct. 28, 1985,

*Assistant Professor, Department of Mechanical and Aerospace Engineering. Member AIAA.

Although the importance of the shock geometry in this context has been noted previously,[11] the unsteady flow treatment as presented here has not appeared before in the published literature. The perturbation scheme used differs from that of Ref. 9 in that the local convection velocities and the speed of sound are not assumed uniform. A simple first-order theory is also presented that allows experimentally determined shock parameters to be used and that can readily be incorporated into existing engineering design systems.

II. Unsteady Cascade Flows with Shocks

General Modeling Aspects

Large fan rotors of the type relevant to this study operate at design speed with supersonic relative flow at a typical span section close to the tip. In this study, we restrict ourselves to a cascade model of such a rotor, as illustrated in Fig. 1, taken at a representative span section. The blades are assumed relatively thin, with zero or slight camber, operating at low angles of attack in supersonic relative flow. The flow component normal to the leading-edge locus is assumed subsonic.

It should be kept in mind that the flow in the actual rotor is transonic and mixed and that the hub regions of the blades operate subsonically. Between the subsonic inboard and the supersonic outboard regions is a region with relative Mach number close to one. Although transonic effects must be expected in this region, both the three-dimensionality of the flow and its unsteadiness help reduce the strength of the transonic effects. However, the mixed nature of the flow in the rotor has a considerable influence on the shock structure and, therefore, also on the aeroelastic stability of the rotor.

The focus of this paper is on the coupling between the mean (steady) shock system and the unsteady motion of the cascade. For cascade configurations representative of current rotors, these shocks are typically reflected once or twice before leaving the blade passages, as illustrated in Fig. 2. In current linearized theories, the shock system is assumed to be fixed and thus does not affect the unsteady blade loading.

When the shock system is moving, however, the points on the blade surfaces where the shocks are reflected oscillate with amplitudes which are of the same order as the unsteady cascade motion. It will be shown that the resultant unsteady loads induced by the shock motion have a strong (first-order) effect on the aeroelastic stability of the cascade. Although we will consider only flows with shocks of weak-to-moderate strength in this paper, these comments also apply to strong shocks. It should be noted that the case where the cascade has a strong (normal) in-passage shock has been considered by Goldstein et al.[12] In this case, the flow downstream of the strong shocks is subsonic and rotational.

A perturbation scheme is presented first, which is similar to that used by Van Dyke[13] to treat nonlinear thickness effects for isolated airfoils oscillating in supersonic flow. Using the solutions to the linearized steady problems as starting points, calculated by the methods of Refs. 5 and 14, the corrections due to blade geometry can then be obtained by solving a nonhomogeneous boundary value problem. The aim here is not to present a comprehensive solution to the problem, but rather to isolate the terms that are of importance from a stability standpoint. Because of the complex three-dimensional shock structure existing in actual rotors (see, for example, Refs. 15-18), a complete solution of the problem must ultimately be based on the methods of computational fluid dynamics.

A simple quasisteady model of the shock motion is also presented (Sec. IV), which when combined with linearized cascade theories is believed to offer an "engineering approximation" to the problem. A similar approach was used by Ashley[19] to treat shock motion in "sub-transonic" isolated wing flutter.

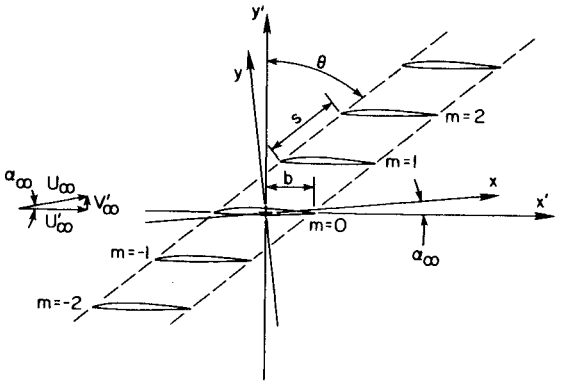

Fig. 1 Cascade geometry and coordinate systems.

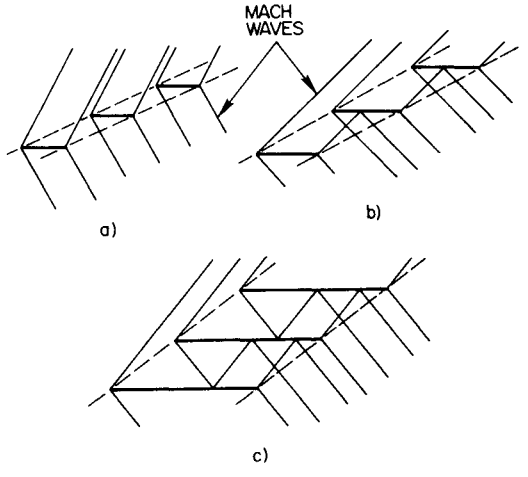

Fig. 2 Reflection patterns for Mach waves and weak shocks: a) no reflections; b) one shock reflection; c) three shock reflections.

Governing Equations

In this study, we restrict ourselves to flows that are irrotational at upstream infinity and free of strong shocks. Within the usual framework of the dynamics of an inviscid perfect gas, the vorticity induced by the shocks is then negligible and a potential exists to second order in a small parameter representative of the flow deflection. The exact equation for this potential is

$$a^2\nabla^2\Phi=\frac{\partial^2\Phi}{\partial t^2}+\frac{\partial}{\partial t}(q^2)+q\cdot\nabla(q^2/2) \tag{1}$$

where a is the local speed of sound and $q=\nabla\Phi$ the local velocity vector. The conservation of total enthalpy and the isentropic formulas yield the additional relations,

$$\frac{\partial\Phi}{\partial t}+\frac{q^2}{2}+\frac{a^2}{\gamma-1}=\frac{U_\infty^2}{2}+\frac{a_\infty^2}{\gamma-1} \tag{2}$$

$$\frac{a^2}{a_\infty^2}=\frac{p}{p_\infty}\cdot\frac{\rho_\infty}{\rho}=\left(\frac{p}{p_\infty}\right)^{(\gamma-1)/\gamma} \tag{3}$$

If the surface of the mth blade is given by the equation

$$B_m(x,y,t)=0 \tag{4}$$

then the boundary condition of tangent flow at the blade surfaces can be written as

$$\frac{DB_m}{Dt}\equiv\frac{\partial B_m}{\partial t}+q\cdot\nabla B_m=0 \qquad m=0,\ \pm1,\ \pm2,\ldots \tag{5}$$

These boundary conditions must be supplemented with radiation conditions at infinity, requiring that the disturbances propagate away from the cascade or rotor in the far field. Across shock waves, conservation of mass and continuity of tangential velocity must be enforced and, across the blades wakes, continuity of pressure and normal velocity are required.

The full potential equation (1) is a reasonable starting point for describing the flow through a compressor rotor, including the effects of shocks, providing the shocks are not too strong. This is the case for large fan rotors, which are most susceptible to flutter, where the blades are thin and relatively sharp-edged and the shocks are oblique and attached to the edges at design speed and low back pressure. The prediction of the actual *location* of the shocks, however, such as their reflection points, may require computational schemes based on the three-dimensional Euler equations in order to yield satisfactory results.

III. Perturbation Approach

For a "tuned" rotor where strict blade-to-blade periodicity exists, the flutter mode is a monochromatic wave traveling in the circumferential direction with respect to the rotor. In locating the linear flutter boundaries, it is therefore sufficient to consider small-amplitude oscillations of the traveling wave form. When the periodicity is broken by imperfections or disorder, the flutter mode is not in general a monochromatic wave. It is always possible, however, to expand an arbitrary traveling wave along a period structure in terms of the individual constant σ modes; see for example Ref. 21.

Consider a two-dimensional infinite cascade model of the rotor, as illustrated in Fig. 1. Let the upper surface on the reference blade in *steady* flow at a small angle of attack α be given by

$$y = -\alpha x + \delta f_u(x) \tag{6}$$

where $\delta \ll 1$ is a measure of the sum of airfoil thickness and camber. Here $\mathcal{O}(\alpha) = \mathcal{O}(\delta)$, so that Eq. (6) is valid to second order in α or δ and the two terms may be combined into one without loss of generality. A similar expression is obtained for the lower surface, substituting f_ℓ for f_u in Eq. (6). Letting the airfoil execute simple harmonic motion with a frequency ω, the instantaneous position of its surface is given by

$$B_0(x,y,t) = y - \delta f(x) - \epsilon g(x) e^{i\omega t} = 0 \tag{7}$$

with an error of third order, $\epsilon^2\delta$, $\epsilon\delta^2$, in δ and ϵ. For convenience, the angle-of-attack term in Eq. (6) has been absorbed into the term $\delta f(x)$ and the subscripts u and ℓ have been dropped with the understanding that Eq. (7) represents two equations, one for each surface. The function $g(x)$ introduced in Eq. (7) defines the motion of the reference blade in the cascade. Since we are retaining only terms linear in the oscillation amplitude, the results for pitching and plunging motions can be determined separately and the results added. Neglecting camber bending and chordwise motion,

$$\begin{aligned} \epsilon g(x) &= -h_0 && \text{in plunge (bending)} \\ &= -(x - ba)\alpha_0 && \text{in pitch (torsion)} \end{aligned} \tag{8}$$

where $x = ba$ defines the location of the pitching axis from midchord. In general, h_0 and α_0 are complex numbers to account for the phase difference between pitching and plunging motions.

Following the analysis of Van Dyke[13] of the isolated airfoil problem, one may write the potential as

$$\Phi(x,y,t)/U_\infty = x + \delta\phi(x,y) + \epsilon\tilde{\phi}(x,y) e^{i(\omega t - \bar{k}M\bar{x})} \tag{9}$$

where the exponential term involving $\bar{k}M\bar{x}$ is introduced for convenience to reduce the equation for $\tilde{\phi}$ to normal form. Here, ϕ represents the perturbation potential corresponding to the mean steady flow and the term involving $\tilde{\phi}$ represents the unsteady perturbation potential about this mean flow.

The governing equations for the perturbation potentials ϕ and $\tilde{\phi}$ can be obtained by substituting Eq. (9) into Eq. (1) and collecting the terms in powers of δ and ϵ. Since ϕ is associated with the steady potential in the limit $\epsilon \to 0$, δ fixed, the steady and unsteady terms can be separated and two equations result. For the mean steady potential, the leading terms become,

$$\begin{aligned} \delta[\phi_{yy} - \beta^2\phi_{xx}] = \delta^2 M^2 [&(\gamma-1)\phi_x(\phi_{xx} + \phi_{yy}) \\ &+ 2\phi_x\phi_{xx} + 2\phi_y\phi_{xy}] + \ldots \end{aligned} \tag{10}$$

valid to second order in δ. For the unsteady perturbation potential about this mean flow, the leading terms become

$$\begin{aligned} \epsilon(\tilde{\phi}_{yy} - \beta^2\tilde{\phi}_{xx} - \nu^2\tilde{\phi}] = \epsilon\delta\Big\{ & M^2[(\gamma-1)(\phi_x\nabla^2\tilde{\phi} + \tilde{\phi}_x\nabla^2\phi) \\ & + 2(\phi_x\tilde{\phi}_x + \phi_y\tilde{\phi}_y)_x] \\ & - i\frac{M^3\nu}{\beta}\Big[(\gamma-1)\Big(2\phi_x\tilde{\phi}_x + \frac{1}{M^2}\tilde{\phi}\nabla^2\phi\Big) \\ & + \frac{2}{M^2}(\phi_x\tilde{\phi}_x + \phi_y\tilde{\phi}_y) + 2\phi_x\tilde{\phi}_x + 2\phi_{xx}\tilde{\phi}\Big] \\ & - \frac{M^2}{\beta^2}\nu^2[2 + (\gamma-1)M^2]\phi_x\tilde{\phi}\Big\} + \ldots \end{aligned} \tag{11}$$

where $\nu = \beta\bar{k}/b$, and $M \equiv M_\infty = U_\infty/a_\infty$. The effect of blade thickness, camber, and angle of attack on the unsteady problem appears through the second-order terms involving products of ϕ and $\tilde{\phi}$. Thus, one must keep the $\mathcal{O}(\epsilon\delta)$ terms, but may discard $\mathcal{O}(\epsilon^2)$ terms, since the latter group does not affect the unsteady lift and moments (although they do affect local pressures).[13] To second order, the $\mathcal{O}(\delta^2)$ terms affect only the steady problem and therefore need not be considered in the present analysis.

If one neglects the right-hand sides of Eqs. (10) and (11), the linearized first-order equations of steady and unsteady supersonic flow are obtained,

$$\phi_{1yy} - \beta^2\phi_{1xx} = 0 \tag{12}$$

$$\tilde{\phi}_{1yy} - \beta^2\tilde{\phi}_{1xx} - \nu^2\tilde{\phi}_1 = 0 \tag{13}$$

for which a number of solution procedures have been developed that are applicable to cascades.[1-5] Using Eqs. (12) and (13) to simplify the right-hand sides of Eqs. (10) and (11), the equations valid to second order in the perturbation potentials become

$$\phi_{yy} - \beta^2\phi_{xx} = 2M^2[\beta^2(N-1)\phi_{1x}^2 + \phi_{1y}^2]_x \tag{14}$$

$$\begin{aligned} \tilde{\phi}_{yy} - \beta^2\tilde{\phi}_{xx} - \nu^2\tilde{\phi} = {} & 2M^2[\beta^2(N-1)\phi_{1x}\tilde{\phi}_{1x} + \phi_{1y}\tilde{\phi}_{1y}]_x \\ & - 2\frac{iM\nu}{\beta}[\beta^2(2N-1)\phi_{1x}\tilde{\phi}_{1x} + \beta^2 N\phi_{1xx}\tilde{\phi}_1 + \phi_{1y}\tilde{\phi}_{1y}] \\ & - 2N\nu^2\phi_{1x}\tilde{\phi}_1 \end{aligned} \tag{15}$$

where $N = (\gamma+1)M^2/2\beta^2$.

The boundary conditions are obtained by substituting Eq. (7) into Eq. (5) and separating steady and unsteady parts. To

second order, neglecting $\mathcal{O}(\epsilon^2)$ terms,

$$\delta\phi_y = \delta f' + \delta^2(f'\phi_x - f\phi_{yy}) \text{ on } y=0^{\pm} \tag{16a}$$

$$\epsilon\tilde{\phi}_y = \epsilon\left[g' + i\frac{\nu\beta}{M}g\right]e^{i\bar{k}M\bar{x}} + \epsilon\delta\left[\left(\tilde{\phi}_x - i\frac{\nu M}{\beta}\tilde{\phi}\right)f' + (g'\phi_x - g\phi_{yy})e^{i\bar{k}M\bar{x}} - f\tilde{\phi}_{yy}\right] \text{ on } y=0^{\pm} \tag{16b}$$

with the upper and lower surface function $f_{u,\ell}$ substituted for f, as appropriate.

The oscillating leading- and trailing-edge shocks introduce certain difficulties that must be overcome for this scheme to work. It is apparent, for example, that delta function singularities will appear in the nonhomogeneous terms on the right-hand side of Eqs. (14) and (15), because of the jump in the flow velocities as the shocks are crossed. Across the shocks, a second-order form of the Rankine-Hugoniot relations must be satisfied, introducing additional complications since the instantaneous shock position depends on the motion. Both problems can be avoided by the same smoothing device used by Van Dyke,[13] which essentially replaced shock waves by very rapid isentropic compressions.

The boundary value problem associated with the first-order problem [Eqs. (12) and (13)] and the first-order terms of the boundary conditions [Eqs. (16)], can be solved by several existing methods.[1-5] In Ref. 5 the problem is recast in the form of a set of dual integral equations involving the upwash $\bar{v}_0(\bar{x})$ and the pressure loading $[\bar{p}_0(\bar{x})]$ on the zeroth blade and its extension to $\pm\infty$,

$$\bar{v}_0(\bar{x}) = \frac{i\beta}{2}\int_{-\infty}^{\infty} G(\tau+\bar{k}M)F_0(\tau+\bar{k}M)e^{i\bar{x}\tau}\,d\tau \tag{17}$$

$$[\bar{p}_0(\bar{x})] = \int_{-\infty}^{\infty} F_0(\tau+\bar{k}M)e^{i\bar{x}\tau}\,d\tau \tag{18}$$

where

$$G(\tau) = \frac{\sqrt{\tau^2-\bar{k}^2}\sin(\bar{s}_2\beta\sqrt{\tau^2-\bar{k}^2})}{(\tau-\bar{k}/M)\,[\cos(\bar{s}_2\beta\sqrt{\tau^2-\bar{k}^2})-\cos(\Omega-\bar{s}_1\tau)]} \tag{19}$$

and F_0 is an unknown function whose determination solves the problem. Note that the upwash $\bar{v}_0(\bar{x})$ is known for $|\bar{x}|<1$, while $[\bar{p}_0(\bar{x})]\equiv 0$ for $|\bar{x}|>1$. For details on the solution of these equations, see Ref. 5.

The second-order solution for the mean steady potential ϕ obtained by solving Eq. (14) leads to the well-known Buseman result,[22] and is not required for the second-order unsteady problem. Now Eq. (15) is a linear nonhomogeneous equation, for which a solution can always be expressed as the solution of the homogeneous equation plus a particular integral,

$$\tilde{\phi} = \tilde{\phi}^c + \tilde{\phi}^p \tag{20}$$

where the complementary solution $\tilde{\phi}^c$ must correct for the boundary condition violations introduced by $\tilde{\phi}^p$, so that the total solution satisfies the second-order flow tangency condition. In principle, a particular integral can always be constructed, since the fundamental solution for the reduced wave equation is known and the appropriate Green's function exists. The remaining boundary value problem for $\tilde{\phi}^c$ can then be solved by existing methods for the first-order problem, after the necessary adjustments to the boundary conditions have been made.

Using the dual integral equation approach, the kernel G in Eq. (19) can be shown to remain unchanged for the second-order problem. This follows from the momentum equation in the y direction, which to second order in the terms involving $\tilde{\phi}$ reads, on the blade surface,

$$\frac{\partial\bar{p}}{\partial y}\cdot e^{i\bar{k}M\bar{x}} = \epsilon\left[\frac{i\bar{k}}{bM}\tilde{\phi}_y - \tilde{\phi}_{xy}\right] + \epsilon\delta\left[\left(\frac{i\bar{k}}{bM}\tilde{\phi}_y - \tilde{\phi}_{xy}\right)_y\cdot f + (\beta^2\phi_x\tilde{\phi}_x - \phi_y\tilde{\phi}_y)_y - g\phi_{xyy}e^{i\bar{k}M\bar{x}}\right] \tag{21}$$

where the derivatives on the right-hand side are evaluated at $y=\pm 0$ and the appropriate upper or lower surface functions are substituted for $f(x)$. Here $\bar{p}(x,y)$ is the nondimensional unsteady perturbation pressure amplitude and second-order terms in ϵ have been neglected. Since the upwash integral, Eq. (17), for the first-order problem is obtained by integrating Eq. (21) from $-\infty$ to x (neglecting the $\epsilon\delta$ terms), it follows that the same type of equation will be obtained for the second-order problem. The reason is that the nonlinear coupling terms in the last bracket are multiplied by $\epsilon\delta$ and thus it suffices to use the first-order solution when evaluating these terms. The coupling terms thus modify the upwash on the reference blade by an amount $\Delta\bar{v}_0$ that can be calculated; thus, for the second-order problem,

$$\bar{v}_0(\bar{x}) = \delta\tilde{\phi}_y - \delta\tilde{\phi}^p_y - \epsilon\delta\Delta\bar{v}_0 \tag{22}$$

where the second-order terms in Eq. (16) are to be taken for $\tilde{\phi}_y$ and $\tilde{\phi}^p_y$. It should be noted that in the second-order problem, two upwash integral equations are obtained, one for the upper and one for the lower surface of the reference blade. In this case, there are two functions $F_0^{\pm}$ to be determined and it is necessary to account for the induced upwash caused by the symmetric part, $p_0(x,0^+)=p_0(x,0^-)$, of the blade pressure distribution.

IV. First-Order Shock Doublet Approximation

Using arguments similar to those advanced by Ashley[19] in his treatment of shock motion in isolated wing flutter, an approximate theory for the effect of shock motion on rotor flutter can be developed. In addition to its relative simplicity, it has the added advantages that it can be incorporated into existing aeroelastic analysis programs and experimentally determined shock parameters and motions can be used. The latter advantage is believed important, as experimental data on rotors suggest that the shock structure is often significantly different from what would be expected from two-dimensional cascade calculations.[15,18] Evidently, the three-dimensional nature of the shock system cannot be ignored when the relative flow is mixed subsonic-supersonic over the blade span.

The basic approach used by Ashley[19] is to take the unsteady airloads as the sum of the loads calculated by linearized theory, plus the contribution of a "shock-force doublet" centered at the shock location. A similar approach is followed here, although there are important differences between the cascade and the isolated airfoil problem that must be taken into account. The most important difference in this context is that in the cascade problem one must deal with shock reflections from adjacent blades. When the blades oscillate, the points on the blade surfaces where the shocks are reflected also oscillate, with amplitude of the same order as the blade motion. The amplitude and phase of this shock motion are strong functions of the interblade phase angle—another variable not found in the isolated airfoil problem.

Consider the reflection of an upward propagating oblique shock by the lower surface of a blade, say the zeroth or reference blade, as illustrated in Fig. 3. From Fig. 2 it is evident that such a shock either originated at the trailing edge of the blade below or is the reflection (by the blade below) of the downward propagating shock from the leading edge of the reference blade. If the blade leading and trailing edges

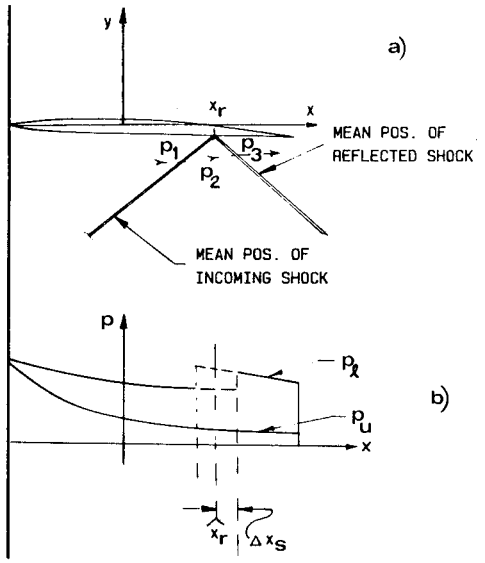

Fig. 3 a) Typical shock reflection; b) resultant pressure jump at reflection point.

are sharp, the shocks are attached and the shock displacements at the edges are essentially instantaneous and in phase with the blade motion there. But because of the finite speed of propagation of the shock there is a time lag between the motions at the origin of the shock and the point at which it is reflected by an adjacent blade. This together with the presence of an interblade phase angle σ results in an important phase difference between the shock-induced aerodynamic loads and the blade motion; and it is this phase difference that determines whether the shock motion is stabilizing or destabilizing.

To first order in the blade amplitudes, the shock strengths may be assumed constant when calculating lifts and moments. If Δx_s is the amplitude of the oscillation of the shock reflection point about the mean steady point x_r, the instantaneous location of the shock reflection point is then

$$x_s(t) = x_r + \Delta x_s e^{i(\omega t - \phi_s)} \tag{23}$$

where ϕ_s is its phase angle with respect to the motion of the reference blade. From Fig. 3b, it follows that the incremental lift and moment per unit span on the reference blade due to the motion of the shock reflection point are

$$L_s = -\Delta p_s \Delta x_s e^{i(\omega t - \phi_s)} \tag{24}$$

$$M_s = x_r \Delta p_s \Delta x_s e^{i(\omega t - \phi_s)} \tag{25}$$

Here $\Delta p_s = p_3 - p_1$ is the total pressure jump across the incoming shock and its mean (steady) reflection point $x = x_r$. Note that L_s and M_s can be interpreted as resulting from oscillating "shock doublets" distributed over the small reflection region (Fig. 3).

It is convenient to express the shock-induced lift and moments in terms of nondimensional lift and moment coefficients. Adopting the conventions and notation of Ref. 5,

$$L = \pi \rho_\infty U_\infty^2 c [C_{Lv} \cdot \bar{v}_b + C_{L\alpha} \cdot \alpha] \tag{26}$$

$$M = \pi \rho_\infty U_\infty^2 c^2 [C_{Mv} \cdot \bar{v}_b + C_{M\alpha} \cdot \alpha] \tag{27}$$

Note that in bending or plunge, the velocity $\bar{v}_b \equiv v_b / U_\infty = -ik\bar{h}$ has been used instead of the displacement $\bar{h} = h/b$. The matrix of incremental lift and moment coefficients due to the shock motion at one reflection point can then be written as

$$\begin{bmatrix} C^s_{Lv} & C^s_{L\alpha} \\ C^s_{Mv} & C^s_{M\alpha} \end{bmatrix} = \pm \frac{\Delta \bar{p}_s}{4\pi} e^{-i\phi_s} \begin{bmatrix} 2\left(\frac{\Delta \bar{x}_s}{\bar{v}_{0b}}\right) & 2\left(\frac{\Delta \bar{x}_s}{\alpha_0}\right) \\ -\bar{x}_r\left(\frac{\Delta \bar{x}_s}{\bar{v}_{0b}}\right) & -\bar{x}_r\left(\frac{\Delta \bar{x}_s}{\alpha_0}\right) \end{bmatrix} \tag{28}$$

Here the + sign is to be used if the shock is reflected from the top (suction) surface and the − sign if it is reflected from the bottom (pressure) surface. After summing the contributions of all shocks and their reflections, the total lift and moment is found by adding the linearized results, calculated in this study by the method of Ref. 5.

The quantities necessary to implement the first-order shock-doublet model can in principle be determined either experimentally or by direct calculations. It should be pointed out that the phase angle ϕ_s in the problem is not plagued by the uncertainties encountered in Ref. 19, but can in fact be calculated with reasonable confidence from first principles. By applying the Rankine-Hugoniot relations, the shock oscillation amplitudes can also be calculated, as illustrated in Refs. 8, 10, 12, and 23. This approach unfortunately defeats the main purpose of the shock-doublet approximation, since it couples the shock motion with the unsteady flowfield. At low reduced frequencies at least, where the shock motion is believed to be most important from a stability standpoint, it seems reasonable to use quasisteady formulas for the motion of the shocks. Such formulas can be derived by assuming that the time required for a shock to propagate a distance of the order of the blade spacing is small compared to the period of oscillation. For the reflection of an upward traveling trailing-edge shock, as illustrated in Fig. 3, the asymptotic relations for the phase and amplitude of the shock reflection point can be written as

$$\left(\frac{\Delta \bar{x}_s}{\bar{v}_{0b}}\right) e^{-i\phi_s} \cong -\frac{i\beta}{k}[1 - e^{-i(\sigma + \bar{k}M\beta\bar{s}_2)}] \tag{29}$$

$$\left(\frac{\Delta \bar{x}_s}{\alpha_0}\right) e^{-i\phi_s} \cong -\beta[1 + \beta\bar{s}_2 - \bar{s}_1 - e^{-i(\sigma + \bar{k}M\beta\bar{s}_2)}] \tag{30}$$

Note the strong dependence on the interblade phase angle σ and the additional phase angle term $\bar{k}M\beta\bar{s}_2$ that arises from the fact that the propagation speed of the shock is finite. Here the speed has been approximated by the freestream speed of sound and the shock direction by the Mach lines. The derivation of these formulas is a straightforward application of the same kinematic ideas used in Appendix E of Ref. 24 to treat Mach wave reflections. The two remaining quantities $\Delta \bar{p}_s$ and $\bar{x}_r$ in Eq. (28) are readily calculated from shock expansion theory and geometric considerations involving the shocks and their reflections, once the blade geometry and angle of attack are specified.

Similar asymptotic relations can be obtained for a leading-edge shock reflected twice, Fig. 2c. At the first reflection (top surface),

$$\left(\frac{\Delta \bar{x}_s}{\bar{v}_{0b}}\right) e^{-i\phi_s} \cong -\frac{i\beta}{k}[1 - e^{i(\sigma - \Delta\phi)}] \tag{31}$$

$$\left(\frac{\Delta \bar{x}_s}{\alpha_0}\right) e^{-i\phi_s} \cong -\beta[1 - \kappa_1 - e^{i(\sigma - \Delta\phi)}] \tag{32}$$

while at the second reflection (bottom surface)

$$\left(\frac{\Delta\bar{x}_s}{\bar{v}_{0b}}\right)e^{-i\phi_s} \cong \frac{-i\beta}{k}[1+e^{-2i\Delta\phi}-2e^{-i(\sigma+\Delta\phi)}] \tag{33}$$

$$\left(\frac{\Delta\bar{x}_s}{\alpha_0}\right)e^{-i\phi_s} \cong \beta[1-2\beta\bar{s}_2-2(1-\kappa_1)e^{-i(\sigma+\Delta\phi)}+e^{-2i\Delta\phi}] \tag{34}$$

where $\Delta\phi = \bar{k}M\beta\bar{s}_2$ and $\kappa_1 = \bar{s}_1 + \beta\bar{s}_2$.

Finally, it should be pointed out that in deriving the incremental lift and moment due to the shock motion, the shocks were treated as step waves and the reflection as regular. Boundary-layer effects would smear out the pressure jump Δp_s as well as affecting the reflection pattern close to the surface (bifurcated shocks may occur). In any event, effective Δp_s and x_r can be defined such that the relations of Eq. (28) hold.

V. Effect of Shocks on Aeroelastic Stability

Two characteristic features of supersonic rotor flutter have proved difficult to explain based on linearized analysis. The first is the favorable influence of pressure ratio at constant rotor speed. Thus, lowering the rotor operating line reduces the flutter speed and vice versa. Since this effect appears to be caused by blade loading, it cannot be accounted for by cascade theories that linearize about the undeflected flow.

The second characteristic feature is the extreme steepness of the flutter boundary. While some aeroelastic instabilities in turbomachinery rotors are "soft," this one is not: The vibratory stress is observed to increase rapidly with increasing Mach number as the boundary is crossed. Calculations based on linearized cascade theories, on the other hand, predict a less steep boundary. Figures 4 and 5 illustrate this point for single-degree-of-freedom torsional flutter of typical cascades representative of current technology rotors. Note that the strength of the instability (i.e., the amount of negative aerodynamic damping), which here is proportional to the imaginary part of the moment coefficient due to torsion, acutally *decreases* beyond $M \cong 1.5$. Calculations for coupled bending-torsion flutter reveal a similar behavior with respect to Mach number.

Halliwell[11] has also noted this peculiar behavior and has suggested an explanation. For cascade configurations typical of current rotors, a change from the wave reflection pattern of Fig. 2c to that of Fig. 2b occurs at a certain Mach number in the operating range. Halliwell attributes the anomaly to expected discontinuities in the unsteady force coefficients as this Mach number is crossed. In the case of Verdon's cascades A and B, used in generating Figs. 4 and 5, the Mach numbers in question are 1.282 and 1.669, respectively.

It is clear from Figs. 4 and 5, however, that the moment coefficients are continuous at the corresponding Mach

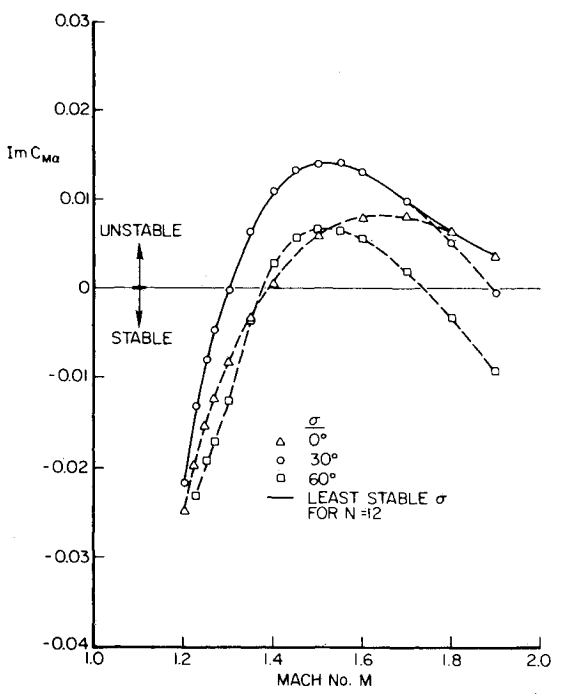

Fig. 4 Imaginary part of moment coefficient due to torsion vs Mach number. Verdon's cascade A: $\theta = 59.5$ deg, $\bar{s}_2 = 0.8$, $k = 0.51$ at $M = 1.4$. Calculated by method in Ref. 5.

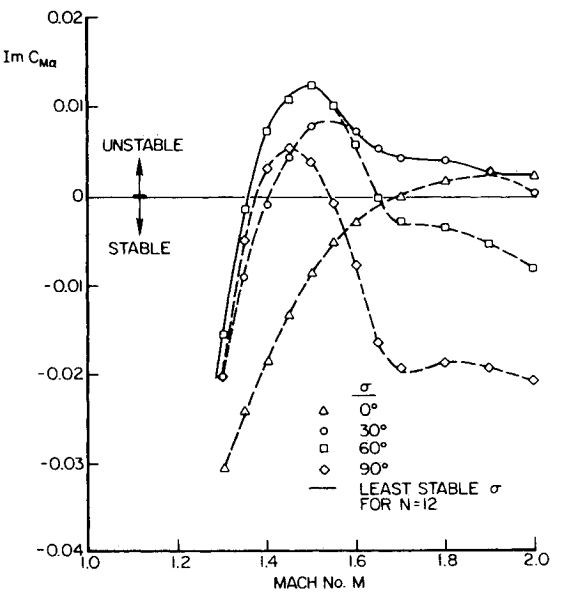

Fig. 5 Same as Fig. 5, for Verdon's cascade B: $\theta = 63.4$ deg, $\bar{s}_2 = 0.6$, $k = 0.65$ at $M = 1.4$.

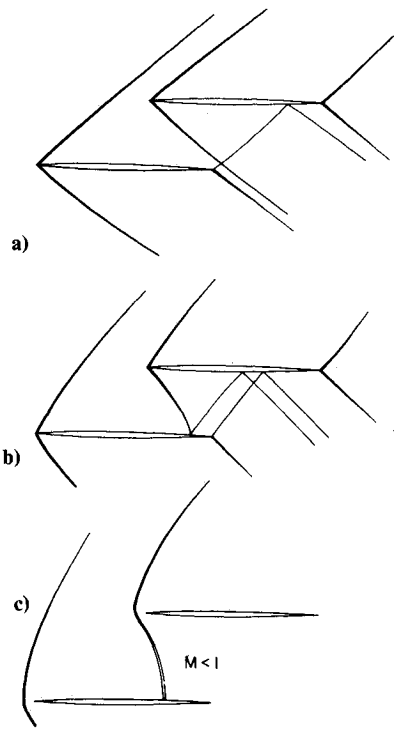

Fig. 6 Expected shock structure at different back pressures for a rotor with Verdon's cascade A typical section: a) low back pressure at design speed; b) moderate back pressure or below design speed; c) high back pressure or low speed (unstarted mode).

numbers. Evidently, the change in stability is gradual and cascade A is *stable* at $M=1.282$ and does not reach peak instability until $M\cong 1.55$. It is interesting to note that cascade B also exhibits peak torsional instability around $M\cong 1.5$ and has, in fact, become stable again for all interblade phase angles except $\sigma\cong 30$ deg as $M=1.669$ is reached. Incidentally, the location of maximum $ImC_{m\alpha}$ vs M is a function of reduced frequency $k=\omega b/U$, in addition to interblade phase angle σ, and decreases as k decreases. Also note that the reduced frequency has been scaled by assuming that U and M are proportional, i.e., $k=k_{\text{ref}}\cdot M_{\text{ref}}/M$, where k_{ref} and M_{ref} are given in the figures.

When the unsteady loads induced by the shock motion are included, the two characteristics of supersonic flutter noted previously can be explained. At low back pressure and angle of attack, the weak oblique leading- and trailing-edge shocks will have patterns similar to the Mach wave reflections shown in Fig. 2. Experimental data from Ref. 18 indicates that the in-passage shock structure is strongly affected by the back pressure and also by the rotor speed. The downward propagating leading-edge shocks appear to be especially sensitive and are often observed at larger angles with the blade pressure surfaces than would be expected from two-dimensional shock relations.[15]

Figure 6 illustrates the expected behavior of the shock structure for a rotor with Verdon's cascade A typical section. Note that *increasing* the rotor back pressure has qualitatively similar effect on the shock structure as *decreasing* the relative Mach number, suggesting that it should be stabilizing. Calculations indicate that increasing the back pressure should be stabilizing on pitching oscillations and destabilizing on plunging oscillations (see the dependence on θ_2 and M_2 in Figs. 7 and 8). When the inlet Mach number is increased, the shock strengths increase and the shock reflection points move aft, contributing to the steep flutter boundary observed experimentally. Incidentally, coupling between bending and torsion plays a very important role here. (See Fig. 10; note strong dependence on $\bar{h}_0/\alpha_0$.)

As is now well established, supersonic cascade theories linearized about the undeflected mean flow predict both single-degree-of-freedom (SDOF) torsional flutter and coupled bending-torsion flutter over a range of cascade operating conditions. Pure bending oscillations, on the other hand, are predicted to be stable. Figure 7 illustrates that the unsteady loads due to shock motion can be sufficiently destabilizing at low reduced frequencies to cause SDOF bending flutter. It is interesting to note that the least stable interblade phase angle is in the range $180<\sigma<360$ deg, corresponding to a backward traveling wave. This characteristic is also observed in the shock-induced bending flutter predicted by the theory of Goldstein et al.[12]

Figure 8 shows the effect of shock motion on the imaginary part of the moment coefficient due to torsion, $ImC_{M\alpha}$, for a typical cascade. In both Figs. 7 and 8 the

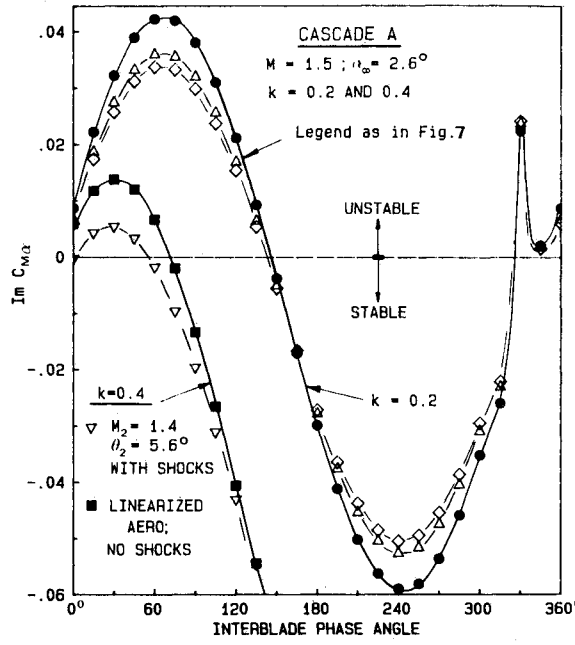

Fig. 8 Typical effect of shock motion on imaginary part of $C_{M\alpha}$ representative of damping in torsion. Verdon's cascade A, as in Fig. 7.

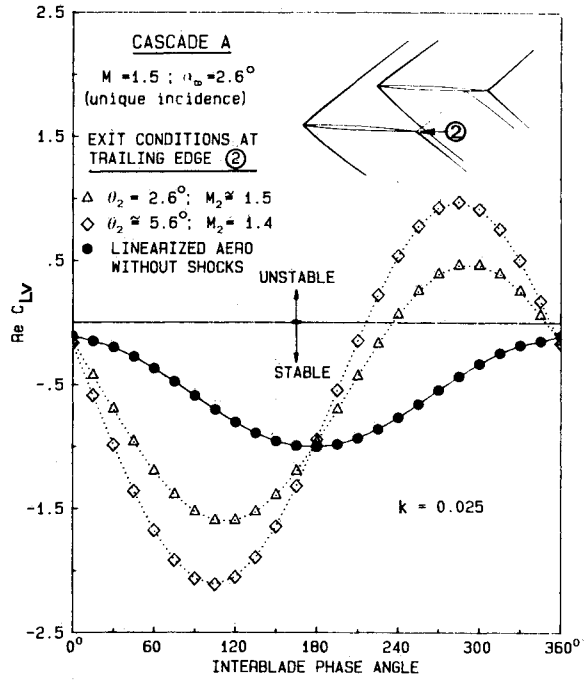

Fig. 7 Typical effect of shock motion on real part of C_{Lv} representative of damping in bending. Verdon's cascade A: symmetric parabolic arc airfoils of 3% maximum thickness; shock-doublet approximation.

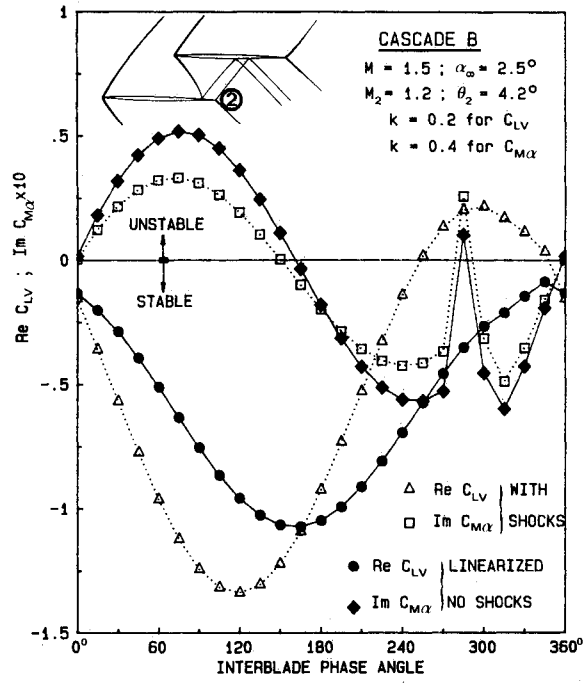

Fig. 9 Typical effect of shock motion on real part of C_{Lv} and imaginary part of $C_{M\alpha}$ for Verdon's cascade B. Blades as in Fig. 7, but note higher reduced frequency for C_{Lv} plot.

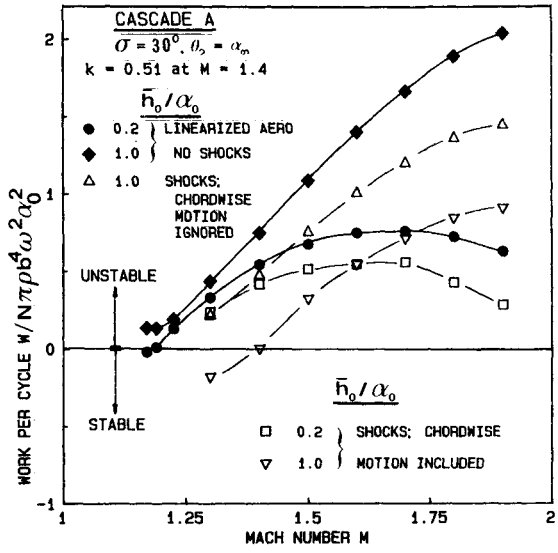

Fig. 10 Typical effect of shock motion on the unsteady aerodynamic work per cycle, per blade, of a coupled bending/torsion flutter mode for a shrouded cascade/rotor.

cascade consists of symmetric, double parabolic arc airfoils with a maximum thickness of 3% of chord, operating at unique incidence. The shock-doublet approximations were used and the mean (steady) shock strengths and geometry were obtained from shock expansion theory, supplemented by the method of characteristics where necessary. It is evident from these results that the shock-induced unsteady aerodynamic loading has a first-order effect on the cascade SDOF flutter boundaries. Figure 9 illustrates the additive effect of several (three) shock reflections, corresponding to the configuration shown in Fig. 2c.

Large fan rotors often have partspan shrouds, which introduce strong coupling between the blade degrees of freedom. Calculations made for the shrouded cascade described in Ref. 20 indicate that the shock-induced loads from the individual degrees of freedom often reinforce each other. Typical results are shown in Fig. 10 in terms of the unsteady aerodynamic work per cycle plotted vs Mach number. The figure reveals an interesting aspect of the coupled problem with shocks: namely, that the effect of *chordwise* blade motion (parallel to the blade chord) is no longer negligible, but must be included.

VI. Conclusions

The following are the main conclusions that can be drawn from this study:

1) The unsteady aerodynamic forces due to shock motion have a pronounced effect on the aeroelastic stability of cascades representative of typical transonic/supersonic rotors and should therefore be included in flutter calculations.

2) Both stabilizing and destabilizing effects are observed. These effects are strong functions of interblade phase angle and shock structure and also depend on reduced frequency and Mach number.

3) The stabilizing effect of back pressure, observed experimentally, can be explained when the effect of shock motion is accounted for.

4) At low reduced frequencies, the shock-induced loads can destabilize bending oscillations sufficiently to cause SDOF bending flutter. The flutter mode is predicted to be a backward traveling wave.

5) Chordwise motion of the blades should be included when modeling the aeroelastic effects of shock motion.

References

[1]Kurosaka, M., "On the Unsteady Supersonic Cascade with a Subsonic Leading Edge—An Exact First Order Theory: Parts 1 and 2," *Transactions of ASME, Journal of Engineering for Power*, Vol. 96, Jan. 1974, pp. 13-31.

[2]Verdon, J. M. and McCune, J. E., "Unsteady Supersonic Cascade in Subsonic Axial Flow," *AIAA Journal*, Vol. 13, Feb. 1975, pp. 193-201.

[3]Nagashima, T. and Whitehead, D. S., "Linearized Supersonic Unsteady Flow in Cascade," British Aeronautical Research Council, R&M 3811, 1978.

[4]Adamczyk, J. J. and Goldstein, M. E., "Unsteady Flow in a Supersonic Cascade with Subsonic Leading-Edge Locus," *AIAA Journal*, Vol. 16, Dec. 1978, pp. 1248-1254.

[5]Bendiksen, O. O. and Friedmann, P., "Bending-Torsion Flutter in Supersonic Cascades," *AIAA Journal*, Vol. 19, June 1981, pp. 774-781. Also see Ref. 24.

[6]Atassi, H. and Akai, T. J., "Aerodynamic and Aeroelastic Characteristics of Oscillating Loaded Cascades at Low Mach Number, Parts I and II," *Transactions of ASME, Journal of Engineering for Power*, Vol. 102, April 1980, pp. 344-356.

[7]Verdon, J. M. and Caspar, J. R., "Subsonic Flow Past an Oscillating Cascade with Finite Mean Flow Deflection," *AIAA Journal*, Vol. 18, May 1980, pp. 540-548.

[8]Strada, J. A., Chadwick, W. R., and Platzer, M. F., "Aeroelastic Stability Analysis of Supersonic Cascades," *Transactions of ASME, Journal of Engineering for Power*, Vol. 101, Oct. 1979, pp. 533-541.

[9]Namba, M. and Minami, R., "Effect of Mean Blade Loading on Supersonic Cascade Flutter," *Proceedings of the 2nd International Symposium on Aeroelasticity in Turbomachines*, Lausanne Institute of Technology, Lausanne, Switzerland, Sept. 1980, pp. 323-332.

[10]Vogeler, K., "A Method of Characteristic Solution for a Finite Oscillating Supersonic Cascade with Thickness Effects," *Proceedings of the 2nd International Symposium on Aeroelasticity in Turbomachines*, Lausanne Institute of Technology, Lausanne, Switzerland, Sept. 1980, pp. 333-347.

[11]Halliwell, D. G., "Some Aerodynamic Considerations in the Prediction of Unstalled Supersonic Flutter in Transonic Fans," *Proceedings of the 2nd International Symposium on Aeroelasticity in Turbomachines*, Lausanne Institute of Technology, Lausanne, Switzerland, Sept. 1980, pp. 309-322.

[12]Goldstein, M. E., Braun, W., and Adamczyk, J. J., "Unsteady Flow in a Supersonic Cascade with Strong In-Passage Shocks," *Journal of Fluid Mechanics*, Vol. 83, Pt. 3, Nov. 1977, pp. 569-604.

[13]Van Dyke, M., "Supersonic Flow Past Oscillating Airfoils Including Nonlinear Thickness Effects," NACA Rept. No. 1183, 1953.

[14]Bendiksen, O. O., "A Uniformly Valid Asymptotic Solution for Unsteady Subresonant Flow Through Supersonic Cascades," *AIAA Journal*, Vol. 22, Jan. 1984, pp. 154-157.

[15]Prince Jr., D. C. , "Three-Dimensional Shock Structures for Transonic/Supersonic Compressor Rotors," *Journal of Aircraft*, Vol. 17, Jan. 1980, pp. 28-37.

[16]McDonald, P. W. et al., "A Comparison Between Measured and Computed Flow Fields in a Transonic Compressor Rotor," *Transactions of ASME, Journal of Engineering for Power*, Vol. 102, Oct. 1980, pp. 883-889.

[17]Wright, L. C. et al., "High-Tip-Speed, Low Loading Transonic Fan Stage," NASA CR-121095, April 1973.

[18]Wuerker, R. F. et al., "Application of Holography to Flow Visualization Within Rotating Compressor Blade Row," NASA CR-121264, Feb. 1974.

[19]Ashley, H., "Role of Shocks in the 'Sub-Transonic' Flutter Phenomenon," *Journal of Aircraft*, Vol. 17, March 1980, pp. 187-197.

[20]Bendiksen, O. O., "Effect of Structural and Damping Nonlinearities on Flutter of Shrouded Fans," AIAA Paper 84-0990, May 1984.

[21]Bendiksen, O. O., "Aeroelastic Stabilization by Disorder and Imperfections," Paper 583P presented at XVI IUTAM International Congress of Theoretical and Applied Mechanics, Lyngby, Denmark, Aug. 1984.

[22]Buseman, A., "Aerodynamischer Auftrieb bei Überschallgeschwindigkeit," *Luftfahrtforschung*, Bd. 12, No. 6, Oct. 3, 1935, p. 213 (see also *Aerodynamics of High Speed*, edited by G. F. Carrier, Dover Publications, New York, 1951, p. 134).

[23]Teipel, I., "Die Berechnung instationärer Luftkräfte im schallnahen Bereich," *Journal de Mecanique*, Vol. 4, No. 3, Sept. 1965, pp. 335-360.

[24]Bendiksen, O. O. and Friedmann, P. P., "Coupled Bending-Torsion Flutter in Cascades with Application to Fan and Compressor Blades," University of California, Los Angeles, CA, Rept. ENG-80-72, Aug. 1980.